GKSS
FORSCHUNGSZENTRUM
in der HELMHOLTZ-GEMEINSCHAFT

Final Draft
of the original manuscript:

Liang, J.; Srinivasan, P.B.; Blawert, C.; Dietzel, W.:
Comparison of electrochemical corrosion behaviour of MgO and ZrO2 coatings on AM50 magnesium alloy formed by plasma electrolytic oxidation
In: Corrosion Science (2009) Elsevier

DOI: 10.1016/j.corsci.2009.06.034

Comparison of electrochemical corrosion behaviour of MgO and ZrO_2 coatings on AM50 magnesium alloy formed by plasma electrolytic oxidation

J. Liang, P. Bala Srinivasan*, C. Blawert, W. Dietzel
Institute of Materials Research
GKSS-Forschungszentrum Geesthacht GmbH
D-21502 Geesthacht, Germany

*Corresponding Author (bala.srinivasan@gkss.de);
Phone: 00-49-4152-871997; Fax: 00-49-4152-871960

Keywords
Magnesium alloy; plasma electrolytic oxidation; corrosion resistance; EIS.

Abstract
Two types of PEO coatings were produced on AM50 magnesium alloy using pulsed DC plasma electrolytic oxidation process in an alkaline phosphate and acidic fluozirconate electrolytes, respectively. The phase composition and microstructure of these PEO coatings were analyzed by X-ray diffraction (XRD) and scanning electron microscopy (SEM). The corrosion behaviour of the coated samples was evaluated by open circuit potential (OCP) measurements, potentiodynamic polarization tests, and electrochemical impedance spectroscopy (EIS) in neutral 0.1 M NaCl solution. The results showed that PEO coating prepared from alkaline phosphate electrolyte consisted of only MgO and on the other hand the one formed in acidic fluozirconate solution was mainly composed of ZrO_2, MgF_2. Electrochemical corrosion tests indicated that the phase composition of PEO coating has a significant effect on the deterioration process of coated magnesium alloy in this corrosive environment. The PEO coating that was composed of only MgO suffered from localized corrosion in the 50 hour exposure studies, whereas the PEO coating with ZrO_2 compounds showed a much superior stability during the corrosion tests and provided an efficient corrosion protection. The results showed that the preparation of PEO coating with higher chemical stability compounds offers an opportunity to produce layers that could provide better corrosion protection to magnesium alloys.

1. Introduction
More attention is being paid, in recent times, to magnesium and its alloys for a wide range of industrial applications, e.g. automotive, aerospace and communication, etc., owing to their low density, high strength to weight ratio, high dimensional stability, good electromagnetic shielding and damping characteristics, and good machining and recycling ability [1-2]. Unfortunately, magnesium alloys, in general, exhibit a poor corrosion resistance, which is primarily attributed to the high chemical activity of magnesium and the lack of a protective passive oxide film [3]. This disadvantage is restricting its widespread use in the aforementioned applications, especially in aggressive environments [4].

In order to improve the corrosion resistance of magnesium alloys, it is necessary to employ proper surface treatments to produce anti-corrosion protection films on the substrate. In the past several decades, many surface modification techniques have been developed for the protection of these alloys, which include electrochemical plating, conversion coatings, anodizing, gas-phase deposition processes, laser surface alloying and organic coatings [5]. Among these techniques, anodizing is one of the most popular methods to provide protection to magnesium alloys [5-7]. Based on the principle of anodizing, a relatively new process, called plasma electrolytic oxidation (PEO), has also been developed in the last decade [8, 9]. By the PEO process, a relatively thick, compact and less porous oxide coating than conventional anodizing can be produced on the surface of magnesium alloys to improve their corrosion resistance remarkably [10-12]. The PEO coatings were found to be mainly composed of magnesium oxide with some of other electrolyte-borne elements (Mg_2SiO_4, $Mg_3(PO_4)_2$ or $MgAl_2O_4$, etc.) [13-15]. For some applications, these PEO coatings cannot provide sufficient corrosion protection to the substrate especially during long term exposures, if the environment is aggressive, as some of the constituents of the oxide coating are not stable in neutral and acidic environments [16,17]. Thus, many attempts have been made to produce PEO coatings with more stable oxides and compounds by modifying the constituents of the electrolytes [18-23]. However, most of these investigations seemed to change the composition of PEO coating only to a small extent and magnesium oxide still remains as the main phase. Recently, Yao, et al. [24] found that the MAO coating which was composed of t-ZrO_2 and c-ZrO_2 could be produced on AZ91D magnesium alloy in a zirconate electrolyte. Mu, et al. [25] also reported that MgF_2/ZrO_2 composite PEO coating was prepared on pure magnesium. The distinct characteristic feature of this PEO coating was that its phase composition mainly consisted of relatively inert compounds (ZrO_2 and/or MgF_2) without MgO or with a little of MgO. This kind of PEO coating was expected to be beneficial to providing a favorable long term protection to magnesium alloys. In order to confirm this hypothesis, in the present investigation two kinds of PEO coatings with different phase composition, i.e. one coating with predominantly MgO phase and the other coating with predominantly ZrO_2 phase were prepared on an AM50 magnesium alloy. Their corrosion/deterioration processes were investigated systematically by electrochemical techniques, and an attempt to correlate the microstructure and phase composition of PEO coatings with the corrosion behaviour was made.

2. Experimental

Coupons of size 15 mm × 15 mm × 4 mm from an AM50 magnesium alloy (mass fraction: 4.4 to 5.5% Al, 0.26 to 0.6% Mn, max 0.22% Zn, max 0.1% Si, and Mg balance) were used as the substrate in this investigation. The specimens were ground with different grit (up to 2500 grit) emery sheets before the PEO treatment.

The plasma electrolytic oxidation processes were carried out using a pulsed DC power source with a frequency of 50 Hz in alkaline phosphate electrolytic solution and acidic fluozirconate electrolytic solution, respectively. During the PEO process, the magnesium alloy sample and the wall of the stainless steel container were used as the anode and cathode, respectively. The alkaline phosphate electrolytic solution was prepared from the solution of Na_3PO_4 (8 g/l) in distilled water with an addition of NH_4OH (18 g/l). The formation of the oxide coatings was achieved at a constant current density of 30 mA/cm^2 for 10 minutes. The fluozirconate electrolytic solution was prepared from the solution of K_2ZrF_6 (3.0 g/l) in distilled

water with an addition of NaH_2PO_2 (1.0 g/l). To get the PEO coating on magnesium alloy in the acidic fluozirconate electrolytic solution successfully, a primary flash coating was prepared firstly in alkaline phosphate electrolytic solution to inhibit anodic dissolution of the magnesium alloy in this solution at the initial stage of processing. Because it is difficult to keep the constant current density in this solution during PEO process, the formation of the oxide coatings was achieved at a constant voltage of 420 V for 10 min. The temperatures of both PEO electrolytes were kept at 23 ± 2˚C with the use of a cooling system. All coated samples were rinsed thoroughly in water and dried in ambient air after PEO the processes were finished.

The surface roughness of the coatings was assessed using a Hommel profilometer. X-ray diffraction (XRD) was performed using a Philips PW1820 diffractometer with Cu Kα radiation to determine the phase composition of the PEO coatings. Scanning electron microscopy (Cambridge Stereoscan) was used to examine the surface morphology of the PEO coatings which were sputtered with thin gold films in order to prevent surface charging effects. Elemental line scan in the cross-section of PEO coatings was measured by Zeiss Ultra 55 scanning electron microscopy equipped with energy dispersive X-ray.

Electrochemical tests were carried out using a computer controlled potentiostat/frequency response analyser (Gill AC, ACM Instruments, UK) to evaluate the corrosion behaviour of the PEO coatings. A typical three electrode cell, with the coated samples as working electrode (0.5 cm^2 exposed area), the Ag/AgCl electrode (saturated with KCl) as reference electrode, and a platinum mesh as counter electrode, was used. All electrochemical tests were conducted in triplicate in 0.1 M NaCl solution with pH of 7 in order to ensure the reproducibility of results. The measurement of open circuit potential with time (OCP-t) was performed to understand the degradation of coatings based on the changes in potential during the exposure to the corrosive electrolyte. Potentiodynamic polarization tests were performed at a scan rate of 0.5 mV/s on the coated samples after exposure periods of 0.5, 24 and 50 hours, respectively. Electrochemical impedance spectroscopy (EIS) tests were performed at the open circuit potential with an AC amplitude of 10 mV over the frequency range from 30,000 Hz to 0.01 Hz, and the measurements were made after 0.5, 2, 5, 10, 25 and 50 hours of immersion in the test electrolyte.

3. Results

3.1 Phase composition and microstructure

X-ray diffraction (XRD) analyses were used to investigate the chemical composition of the PEO coatings prepared from the two different electrolytes. The XRD pattern, as shown in **Figure 1(a)**, reveals that the PEO coating produced in alkaline phosphate electrolyte was mainly composed of MgO. Interestingly, chemical compounds associated with the phosphate, the main anions composition in electrolytic solution were not detected in the coating. Instead, a broad amorphous peak could be identified in the XRD pattern in the range 2θ = 20° to 35°, which suggested the plausible existence of phosphate in amorphous form in PEO coating. For the PEO coating prepared in acidic fluozirconate electrolytic solution, it can be seen from **Figure 1(b)** that the characteristic peaks of tetragonal ZrO_2 (*t*-ZrO_2) and monoclinic ZrO_2 (*m*-ZrO_2) phases were pronounced. In addition, a few peaks corresponding to MgF_2 with very little of MgO were also detected. These results indicate that the constituents of fluozirconate from the electrolyte participated in the plasma thermo-chemical reactions during the PEO process and

were incorporated into the coating as compounds. For both PEO coatings, the diffraction peaks of Mg corresponding to the substrate were detected. Based on the main phase composition of the PEO coatings identified in XRD, the alkaline phosphate and acidic fluozirconate coatings are addressed as "MgO" and "ZrO_2" coatings, respectively, in the following discussions. In the MgO coating

The surface and cross-section morphologies of the MgO and ZrO_2 coatings are shown in **Figure 2**. The typical surface morphology of the MgO coating presented in Figure 2(a) reveals many micropores and some cracks in the surface. The mean surface roughness (R_a) of this coating was 2.2 ± 0.2 μm. The features observed in the cross-section of this coating suggest that not all the micropores were through-going into the interior and appeared to be sealed or partially-sealed internally (Figure 2(b)). The ZrO_2 coating, Figure 2(c), had a different surface appearance compared to the MgO coating. Two distinct characteristics were identified clearly on the surface. One was the so-called sintered protrusions with relatively large-sized micropores (regions A in Figure 2(c)), and the other was the surface with numerous smaller micropores (regions B in Figure 2(c)). Due to the above morphological features, the surface of the ZrO_2 coating was very rough and this was confirmed by the roughness measurements (R_a = 3.6 ± 0.6 μm).

The cross-section morphology of the MgO coating shown in Figure 2(b) reveals clearly that the major part of the coating was relatively compact, even though some defects were observed in the inner regions of the coating. In the cross-section of the MgO coating spherical pores were observed, some of which were filled with coating compounds, and a few others were like gas bubbles. The thickness of the coating was around 28 ± 5 μm. The globular shaped pores filled with the coating compounds and an hair-line crack (sectioned portion of an inter-connecting pore) are marked as (i) and (ii), respectively, in this micrograph. On the other hand, the thickness of the ZrO_2 coating was around 40 ± 8 μm (Figure 2(d)). Unlike the case of the MgO coating, the cross-section of the ZrO_2 coating contained relatively large irregular-shaped pores and micro-cracks which are marked as regions (i) and (ii), respectively, in Figure 2(d). In addition, a few circular and irregular-shaped pores of different sizes were also observed in this coating.

The elemental distribution obtained by EDS line scan in cross-section of PEO coatings are shown in **Figure 3**. The elements O, Mg, P and very little of Al were detected in the coating formed in the MgO coating (Figure 3(a)). While the P concentration increased in the inner part, the concentrations of O and Mg were relatively uniform throughout the cross-section of this coating; For the specimen treated in acidic fluozirconate electrolytic solution (ZrO_2 coating), the elements of O, F, Mg, P and Zr were present throughout the coating (Figure 3(b)). The concentrations of O, P and Zr were relatively uniform in the coating according to the scanning line. Enrichment of F near to the coating/substrate interface was not obviously negligible, although F concentration was also uniform in the rest of the regions. From the EDS spectra it appears that in the MgO coating the coating/substrate interface is slightly enriched with P. Even though the magnesium phosphate phase was conspicuously absent in this coating, the formation of an amorphous phase rich in phosphate could not be ruled out. However, it could not be confirmed in this investigation. In the case of ZrO_2 coating, the interface seems to have been slightly enriched with F, suggesting the formation of MgF_2 during the initial stages of PEO process.

3.2 Corrosion Studies

The measurement of open circuit potential (OCP) as a function of immersion time is used to study some aspects of the chemical stability and corrosion process of the surface layers on the magnesium alloy [26]. The OCP curves of the MgO and ZrO_2 coatings are shown in **Figure 4**. For comparison, the OCP of uncoated AM50 magnesium alloy was also recorded and presented in the same figure. It can be seen that the MgO coating, marked "a", showed a relatively more active potential in the initial stages of immersion. Even though the OCP was slowly drifting towards the noble side during the initial 10 hours of exposure, thereafter a fluctuation stage of the corrosion potential was observed in the range from -1490 mV to -1540 mV (vs. Ag/AgCl), which was roughly consistent with the OCP of uncoated magnesium alloy (marked "c"). This indicated that the MgO coating had plausibly failed after about 10 hours of exposure to the electrolyte. The OCP of the ZrO_2 coated specimen was found to reach a value of approximately -1450 mV vs. Ag/AgCl in 0.5 h. After about 5 hours of immersion, a slight shift in OCP was noticed towards the active side and then it shifted towards the noble side again. No further drift of the OCP towards the active side was noticed during the remaining immersion time, indicating that the ZrO_2 coating possessed a higher stability in this corrosive environment.

The corrosion behaviour of these PEO coatings evaluated by potentiodynamic polarization technique in 0.1 M NaCl solution at different immersion times is shown in **Figure 5**. Corrosion potential (E_{corr}), corrosion current density (i_{corr}) and breakdown potential (E_{bd}) derived from these curves are summarized in **Table 1** and **Table 2**, respectively. For comparison, the polarization behaviour of bare magnesium alloy (immersed for 0.5 h) was also assessed and is presented in the same figure. The specimen in the untreated condition registered a free corrosion potential of -1470 mV vs. Ag/AgCl and a corrosion current density of 15 $\mu A \cdot cm^{-2}$. From Figure 5(a) and Table 1, it can be seen that the MgO coating tested after 0.5 hours of exposure to the corrosive environment showed a relatively lower corrosion current density compared to the rest of the conditions, registering a breakdown potential of -1400 mV vs. Ag/AgCl. With prolonged immersions in 0.1 M NaCl solution (24 and 50 hours), the corrosion current density values were found to increase evidently. The rapid increase in current density in the anodic branch of the polarization curves suggests that the breakdown potential is very close to the corrosion potential (E_{corr}).

For the ZrO_2 coating, the corrosion current density was almost one order of magnitude higher than that of the MgO coating in the test performed after 0.5 hours of immersion as can be noticed in Figure 5(b) and Table 2. Unlike in the case of MgO coatings, the corrosion current density values recorded after 24 and 50 hours of immersion were only marginally higher than that registered in the test after 0.5 h of immersion. The breakdown potentials after all three immersion times were around -1350 mV vs. Ag/AgCl, suggesting that there was not much degradation to this ZrO_2 coating even after 50 hours of immersion. The polarization behaviour of these PEO coatings was basically consistent with the records of the OCP and it suggested that even though the MgO coating could offer a better general corrosion resistance in short term immersion process, it was more susceptible to failure than the ZrO_2 coating in neutral NaCl solutions in the relatively long term exposures.

In order to further understand the corrosion behaviour and the associated deterioration process of the MgO and ZrO_2 coatings, electrochemical impedance

spectroscopy (EIS) was employed. **Figure 6** shows the resulting EIS plots of the magnesium substrate with MgO coating obtained after 0.5, 2, 5, 10, 25 and 50 hours of exposures. Analyses of these EIS plots suggest that two different equivalent circuit models are required to fit the results (**Figure 7**). A two time constant model (Figure 7(a)) is appropriate for earlier stages of the corrosion process (0.5 to 10 hours of immersion). The deterioration of the MgO coating in the latter stages (25 to 50 hours of immersion) required the fitting of the plots with one time constant with an additional inductive circuit element (Figure 7(b)). In the equivalent circuits, R_s is the solution resistance, R_p is the resistance of the PEO coating paralleled with constant phase element $(CPE)_p$, R_i is the coating/substrate interface resistance in parallel with $(CPE)_i$, R_f is the resistance of the film formed on the magnesium substrate exposed to the corrosive electrolyte in parallel with $(CPE)_f$, and R_L is the charge transfer resistance of pitting corrosion in series with the inductance L. The EIS plots were fitted with these equivalent circuits with the fitting results shown in Figure 6 as solid lines, and the values of the fitting circuit elements are summarized in **Table 3** and **Table 4**. It can be seen that the EIS plots and the fitting results clearly illustrate the deterioration processes of the MgO coating in the 50 hours immersion tests.

After the initial 0.5 hours of immersion, the MgO coating exhibited relatively high R_p and R_i. The high values of resistances show that both the porous region and interface of the MgO coating provided an effective corrosion protection at the beginning of the immersion process, consistent with the polarization behaviour shown in Figure 5(a). After 2 hours of immersion, both the R_p and R_i decreased remarkably, indicating that the MgO coating had started to partially deteriorate, and with an exposure of 5 hours, the resistances R_p and R_i decreased still further. Between 5 and 10 hours, the deterioration was very low and the resistances of R_p and R_i registered only a marginal drop. As was observed in the OCP measurements, the MgO coating was found to deteriorate drastically after 10 hours of immersion and this was reflected in the impedance behaviour, too, as is evidenced by the presence of an inductive loop in the tests performed after 25 and 50 hours of immersion. It appears that after 25 hours of exposure, the MgO coating did not provide corrosion protection anymore. Hence, using the model proposed in Figure 7(b), the resistances R_p and R_i were represented by the resistance of R_f in 25 and 50 hours of immersion impedance data. The appearance of inductive loops in the low frequency regions of the Nyquist plots is attributed to the localized corrosion damage of the magnesium alloy substrate **[27]**.

For the ZrO_2 coating, however, a totally different EIS behaviour was observed during the 50 hours immersion tests as can be seen from **Figure 8**. Based on the EIS plots, an appropriate equivalent circuit was proposed (**Figure 9**), in which a Warburg element was also included to accurately fit the data. This Warburg element suggested partial control of corrosion by diffusion of electrolyte within the PEO coating **[27]**. The fit results obtained based on this equivalent circuit are given in Figure 8 as solid lines. The derived electrochemical parameters presented in **Table 5** show a higher resistance value of R_i but a relatively low value of R_p at the beginning of the immersion process (0.5 hours), which suggested that R_i had the main effect on the corrosion protection of the magnesium alloy while R_p did not significantly contribute to the corrosion protection, as a consequence of higher degree of defects in the outer porous region. It should also be noted that the values of resistances R_p and R_i at the initial immersion process (0.5 hours) were much lower than those obtained with MgO coating, consistent with the polarization behaviour mentioned earlier in the text. After that, the value of R_p decreased to

very low values with the immersion time while the resistances of R_i maintained higher values along all the immersion process. In addition, the resistances of Z_w were in the range from 5 kΩ·cm^2 to 9 kΩ·cm^2, indicating that the diffusion influence of corrosive electrolyte was relatively steady in the whole immersion process.

The corroded surfaces (0.5 cm^2 area) after EIS tests in 0.1 M NaCl solution revealed further the different corrosion characteristics between the MgO coating and the ZrO_2 coating as shown the micrographs in **Figure 10** and **Figure 11**, respectively. The macroscopic photograph depicted in Figure 10(a) shows that the MgO coating suffered evident corrosion damage after 50 hours of immersion in 0.1M NaCl solution. Severe localized corrosion attack can clearly be observed on the coating surface (region (b) in Figure 10(a)). The higher magnification SEM micrograph in Figure 10(b) showed that these damaged regions were swelled and had corrosion products on it. At the same time, relatively slight corrosion damage occurred in some other regions of this exposed area (Figure 10(c)) and interestingly, the corrosion damage was confined mostly to the micropores. Much different from the morphologies discussed previously for the MgO coating before corrosion testing (Figure 2a), the original micropores were damaged and seemed to be filled with corrosion products. In case of the ZrO_2 coating, however, the macroscopic photograph shown in Figure 11(a) revealed that there was no evident corrosion damage in this PEO coating even after 50 hours of immersion. The higher magnification SEM micrograph shown in Figure 11(b) also demonstrated that the surface microstructure did not undergo any major changes compared to that observed before exposure to the corrosive environment.

4 Discussion

Based on the examination of surface and cross-section morphologies, characteristics of the corroded surface and the electrochemical corrosion results, the evolution of the deterioration processes of the MgO and the ZrO_2 coatings in 0.1 M neutral NaCl solution could be explained as follows:

For the MgO coating on AM50 magnesium alloy, the deterioration process could be divided into two stages according to the EIS behaviour and OCP measurements as a function of immersion time, i.e. degradation during immersion times up to 10 hours and immersion time over 10 hours, respectively. When the immersion time was short, for example, 0.5 hours, corrosive electrolyte penetrated the PEO coating through the micropores in the outer porous region, reaching the inner region/interface. The low corrosion current density value registered in the polarization tests indicated that the MgO phase in the PEO coating was stable at this instance of time, and the flow of current was essentially due to the dissolution of small areas of magnesium substrate exposed to the electrolyte through the pores. The high pore resistance registered in the EIS measurements after 0.5 hours of immersion corroborates the above observation. With prolonged exposure, the corrosion damage of the PEO coating also started to occur, due to the chemical instability of MgO in this test electrolyte. The disintegration of magnesium oxide was reported to occur in neutral chloride solutions in literature **[26, 28-29]**. In the subsequent tests after 2 and 5 hours of immersion, more amounts of the corrosive electrolyte penetrated into the PEO coating through the micropores and the corrosion damage of coating was enhanced as well. After the micropores were permeated by the corrosive electrolyte, the unstable MgO within the micropores hydrated readily with water to form $Mg(OH)_2$ **[28]**. The hydration process of MgO within the micropores probably led to the positive shift of the OCP and kept the

resistance stable during 5 to 10 hours of immersion period, as the formation of $Mg(OH)_2$ plausibly sealed the micropores partially, if not in full **[11,28]**.

As shown in Figure 2(b), there were many interior defects in addition to the outer surface micropores in the PEO coating. It was possible that these micropores and defects overlap randomly each other to form some regions of high defect density in its cross-section. It was also observed that the growth of the PEO coatings was not uniform and there were some localized spots that were covered only by a relatively thin PEO coating with high level of defect density. With an increase in exposure time, it is expected that the corrosion damage of MgO could be high in the micropores and defects, both in the thickness and transverse (lateral) directions of the coating. Consequently, the PEO coating was vulnerable to get destroyed and a higher number of through-going defects were developed in these localized spots. These additional through-going defects favoured the exchange of corrosive electrolyte and corrosion products through the PEO coating, and thereby accelerated the corrosion process within these regions **[26]**. Also, such developed through-going defects can provide an effective pathway for the intrusion of corrosive electrolyte onto the magnesium alloy substrate. As a result, after about 10 hours of exposure, a steep drop and a consequent extensive fluctuation of the OCP were observed (Figure 4(a)). It appears that the fluctuation is on account of the exposure of fresh regions of magnesium substrate to the electrolyte owing to the degradation of coating. The appearance of the inductive loop in the EIS plot after 25 hours of immersion suggested the localized corrosion damage of magnesium alloy substrate after 25 hours of exposure. The through-going defects evolved as the active sites with higher corrosion rate of magnesium alloy substrate, due to the lower resistance to transfer of electrolyte and corrosion products. In this way, the severe localized damage of the PEO coating had resulted in the development of bumped regions on the surface that were constituted with the corrosion products as seen in Figure 10(b).

In the case of the ZrO_2 coating on AM50 magnesium alloy, the large number of fine and open micropores on the coating surface made the penetration of corrosive electrolyte easier and this had led to the exposure of larger areas of the magnesium substrate underneath the coating to the electrolyte. This was reflected by lower resistance values than those of the MgO coating at the initial stage of immersion (0.5 hours). From the point of immersion, the pores were filled with electrolyte and at the bottom of the connecting-pores (near to the coating-substrate interface) corrosion products have formed as a result of dissolution of magnesium substrate. With increasing immersion time, the further penetration of corrosive electrolyte into the PEO coating decreased the resistance of R_p. However, the resistance R_i, which is related to the coating/substrate interface resistance, remained nearly the same throughout the 50 hours immersion period. This is attributable to the fact that the initial dissolution of magnesium substrate and the consequent formation of corrosion products $Mg(OH)_2$ at the inner regions prevented the further exposure of fresh substrate. Moreover, this coating was stable and there were no further opening-ups of pores in the lateral direction in the coating. This was further augmented by the observation of Warburg impedance in the electrochemical circuit, which indicates the slow diffusion controlled corrosion process through the pores. The reason that there had been no pronounced corrosion damage for this PEO coating is attributed to the phase composition of the coating, which consisted of ZrO_2 and MgF_2 having a higher chemical stability in neutral corrosive electrolyte solution. Even though there were small amounts of MgO in the ZrO_2 coating, it is believed that its deterioration was insufficient to

destroy the PEO coating. It can be seen from Figure 11(b) that the 50 hours immersion process did not affect the morphology of the PEO coated surface, which is consistent with this explanation. Due to the fact that the ZrO_2 coating kept its integrity very well during the immersion process, with negligible degree of deterioration, the corrosion current density values in the polarization tests and the resistance values in the EIS tests remained nearly the same. The occurrence of pitting corrosion of magnesium alloy substrate was not observed in the ZrO_2 specimen EIS tested for 50 hours in this chloride electrolyte, as the development and enlargement of local through-going defects due to degradation of PEO coating was negligible. This was demonstrated by the polarization behaviour as well. The MgO coating after 0.5 hours of exposure, showed a pseudo-passive behaviour, showing a breakdown potential of around -1400 mV vs. Ag/AgCl. However, in the tests performed after 24 and 50 hours, the open circuit potential of the MgO specimen was shifted towards the nobler side, and the anodic polarization behaviour was more like the uncoated alloy, showing breakdown close to the open circuit potential itself. On the other hand, the ZrO_2 coated specimen showed nearly the same breakdown potential values of around -1350 mV vs. Ag/AgCl in the polarization tests performed after 0.5, 24 and 50 hours of exposure to the electrolyte. These potential values are roughly 100 mV noble to that of the uncoated alloy, and hence the better pitting resistance observed for the ZrO_2 coatings in the 50 hours impedance tests is justified. Thus, the above observation brings out clearly the fact that the ZrO_2 coating had provided a much superior long-term corrosion resistance to magnesium alloy substrate.

4. Conclusions

1. PEO coatings with different main phase compositions, i.e. MgO and ZrO_2, were prepared by pulsed DC plasma electrolytic oxidation processes in two different electrolytes. While the MgO coating was relatively compact, the ZrO_2 coating had a large volume of fine pores like a sponge.

2. The large fluctuations that were observed in the potential measurement in the 50 hour exposure test depicted the failure of MgO coating. The steep drop and fluctuations in the potential are attributed to the exposure of fresh surfaces of the substrate to the electrolyte due to the damages in the coating. On the other hand, the ZrO_2 coating provided a higher stability in the 50 hours immersion tests as evidenced by stable and nobler potentials throughout the test period.

3. The corrosion resistance of the MgO coating was superior to that of the ZrO_2 coating in the polarization tests after 0.5 hours of exposure to the corrosive environment. However, the corrosion resistance of the MgO coating deteriorated due to prolonged exposure to the test electrolyte as was demonstrated by a localized damage in the tests after 24 hours and 50 hours of exposures. On the other hand, corrosion resistance of the ZrO_2 coating was more or less the same in the polarization tests performed up to 50 hours, which demonstrated the chemical stability of ZrO_2 coating.

4. The 50 hours EIS tests revealed that the deterioration process of the MgO coating on magnesium alloy substrate started from a slow corrosion damage of PEO coating and then progressed finally into a localized corrosion damage of the magnesium alloy substrate. Contrary to the case of the MgO coating, no

corrosion damage of PEO coating and the consequent damage of magnesium alloy substrate were observed in 50 hours immersion tests for the ZrO_2 coating. The EIS results suggested that the PEO coating with relatively stable compounds could provide the long term corrosion inhibiting effect and prevent the localized corrosion of magnesium alloy substrate.

5. The results as a whole clearly suggest that the corrosion resistance of the PEO coating for short-term exposure was predominantly determined by the microstructure/morphology, while the long-term corrosion protection of PEO coating was governed significantly by the synergistic effect of phase composition stability and microstructural integrity in aggressive environments.

Acknowledgements

J. Liang and P. Bala Srinivasan express their sincere thanks to the Hermann-von-Helmholtz Association, Germany and DAAD, Germany for the award of fellowship and funding. The technical support of Mr. V. Heitmann, Mr. U. Burmester and Mr. V. Kree during the course of this work is gratefully acknowledged. The authors acknowledge the support of Dr. Zhiguang Guo, Laboratory of Inorganic Materials Chemistry (CMI), University of Namur (FUNDP), Belgium, in performing the XRD analysis.

References

1. B.L. Mordike, T. Ebert, Mater. Sci. Eng. A 302 (2001) 37.
2. Y. Kojima, Mater. Sci. Forum 350-351 (2000) 3.
3. G. Song, A. Atrens, D. St. John, X. Wu, J. Nairn, Corros. Sci. 39 (1997) 1981.
4. G. Song, A. Atrens, Adv. Eng. Mater. 5 (2003) 837.
5. J.E. Gray, B. Luan, J. Alloys Compd. 336 (2002) 88.
6. Z. Shi, G. Song, A. Atrens, Corros. Sci. 48 (2006) 3531.
7. C. Blawert, W. Dietzel, E. Ghali, G. Song, Adv. Eng. Mater. 8 (2006) 511.
8. A.L. Yerokhin, X. Nie, A. Leyland, A. Matthews, S. J. Dowey, Surf. Coat. Technol. 122 (1999) 73.
9. P. Gupta, G. Tenhundfeld, E.O. Daigle, D. Ryabkov, Surf. Coat. Technol. 201 (2007) 8746.
10. R. Arrabal, E. Matykina, F. Viejo, P. Skeldon, G.E. Thompson, Corros. Sci. 50 (2008) 1744.
11. C. Blawert, V. Heitmann, W. Dietzel, H.M. Nykyforchyn, M.D. Klapkiv, Surf. Coat. Technol. 200 (2005) 68.

12. J. Liang, L. Hu, J. Hao, Appl. Surf. Sci. 253 (2007) 4490.

13. Q. Cai, L. Wang, B. Wei, Q. Liu, Surf. Coat. Technol. 200 (2006) 3727.

14. C.-E. Barchiche, E. Rocca, C. Juers, J. Hazan, J. Steinmetz, Electrochim. Acta 53 (2007) 417.

15. R. Arrabal, E. Matykina, P. Skeldon, G.E. Thompson, A. Pardo, J. Electrochem. Soc. 155 (3) (2008) C101.

16. O. Khaselev, D. Weiss, J. Yahalom, J. Electrochem. Soc. 146 (5) (1999) 1757.

17. G. Song, Corrosion and protection of magnesium alloys, Chemical Industry Press, Beijing, 2006, p. 298 (in Chinese).

18. J. Liang, B. Guo, J. Tian, H. Liu, J. Zhou, W. Liu, T. Xu, Appl. Surf. Sci. 252 (2005) 345.

19. J. Liang, B. Guo, J. Tian, H. Liu, J. Zhou, W. Liu, T. Xu, Surf. Coat. Technol. 199 (2005) 121.

20. H. Duan, C. Yan, F. Wang, Electrochim. Acta 52 (2007) 3785.

21. C. Blawert, V. Heitmann, W. Dietzel, H.M. Nykyforchyn, M.D. Klapkiv, Surf. Coat. Technol. 201 (2007) 8709.

22. J. Liang, L. Hu, J. Hao, Electrochim. Acta 52 (2007) 4836.

23. C.-E. Barchiche, E. Rocca, J. Hazan, Surf. Coat. Technol. 202 (2008) 4145.

24. Z. Yao, H. Gao, Z. Jiang, F. Wang, J. Am. Ceram. Soc. 91 (2) (2008) 555.

25. W. Mu, Y. Han, Surf. Coat. Technol. 202 (2008) 4278.

26. H. Duan, K. Du, C. Yan, F. Wang, Electrochim. Acta 51 (2006) 2898.

27. C.N. Cao, J.Q. Zhang, An Introduction to Electrochemical Impedance Spectroscopy, Science Press, Beijing, 2002, p. 55 (in Chinese)

28. S.J. Xia, R. Yue, R.G. Rateick, Jr., V.I. Birss, J. Electrochem. Soc. 151 (3) (2004) B179.

29. Y. Zhang, C. Yan, F. Wang, W. Li, Corros. Sci. 47 (2005) 2816.

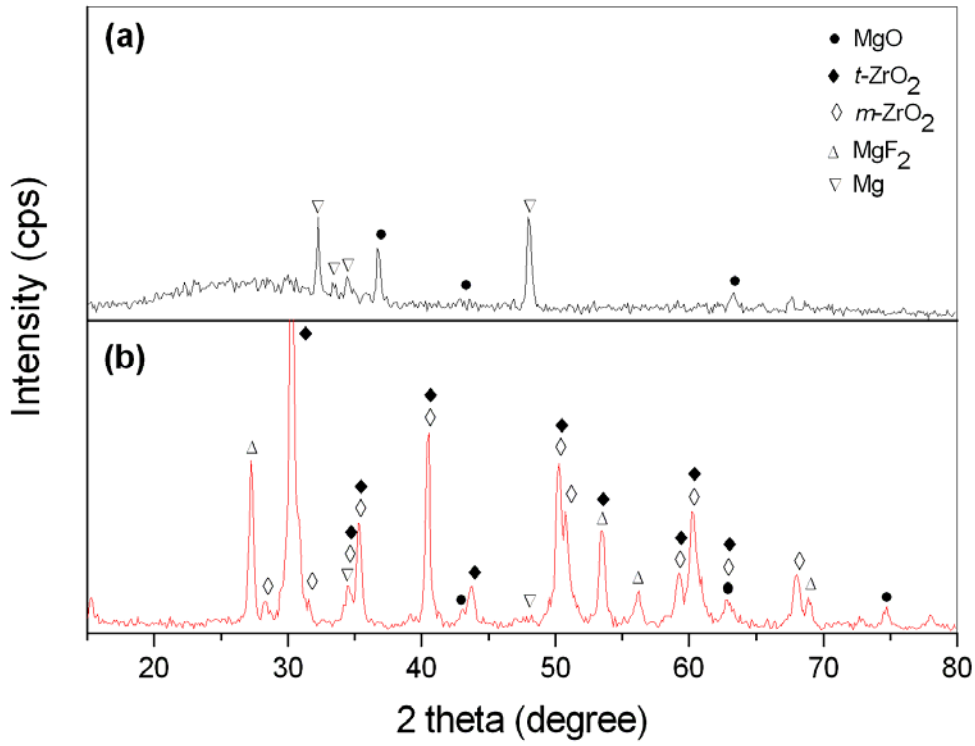

Figure1 XRD patterns of (a) PEO coating formed in alkaline phosphate electrolytic solution and (b) PEO coating formed in acidic fluozirconate electrolyte.

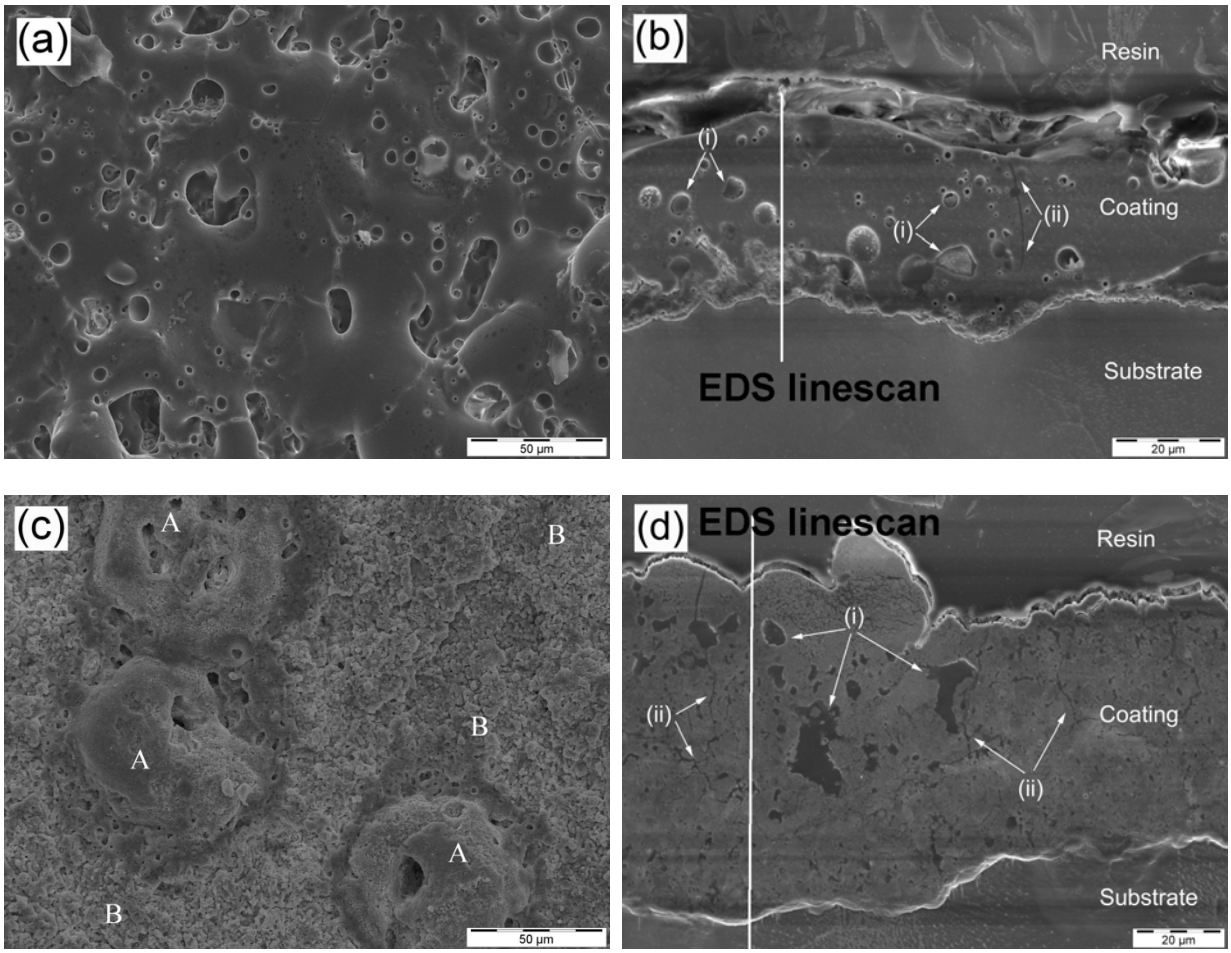

Figure 2 Surface and cross-sectional morphologies of (a, b) MgO coating and (c, d) ZrO_2 coating on magnesium alloy. (i) pores (ii) micro-cracks

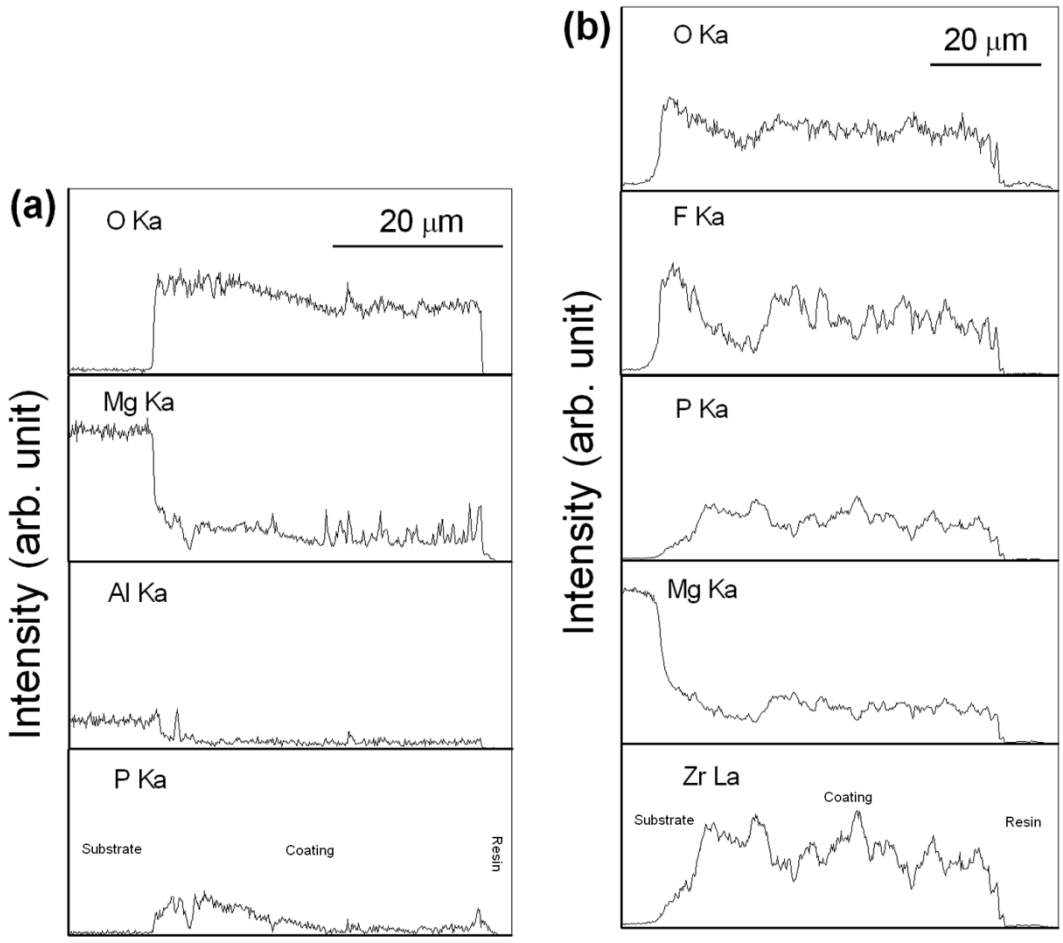

Figure 3 EDS line scan across (a) MgO coating (b) ZrO_2 coating

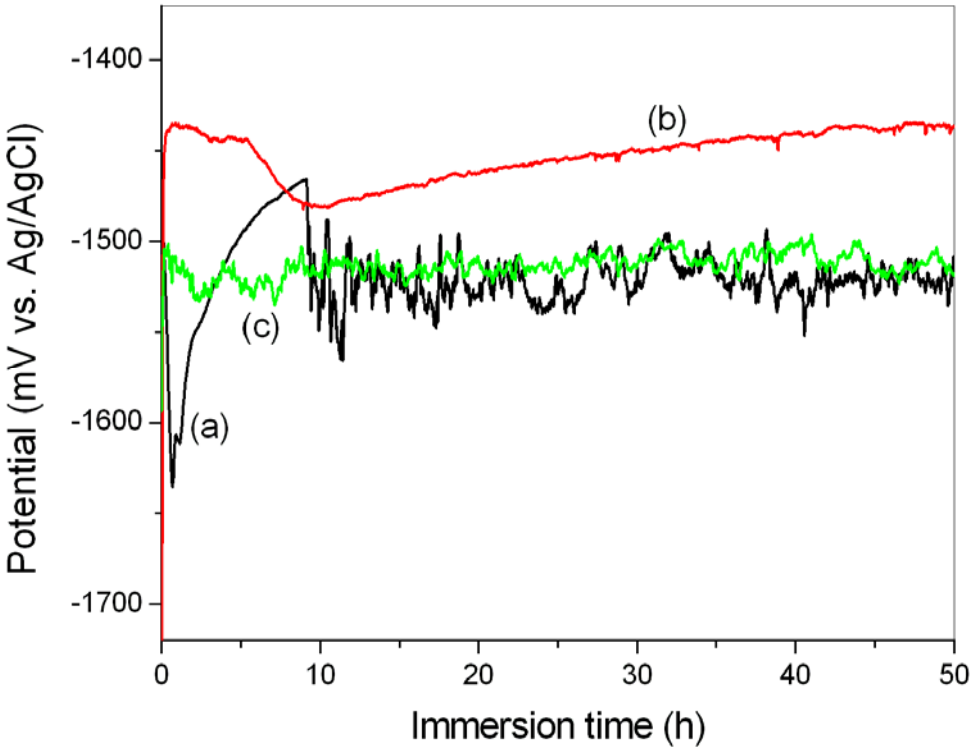

Figure 4 Open circuit potential versus immersion time in 0.1 M NaCl solution: (a) MgO coating, (b) ZrO_2 coating and (c) uncoated AM50 magnesium alloy.

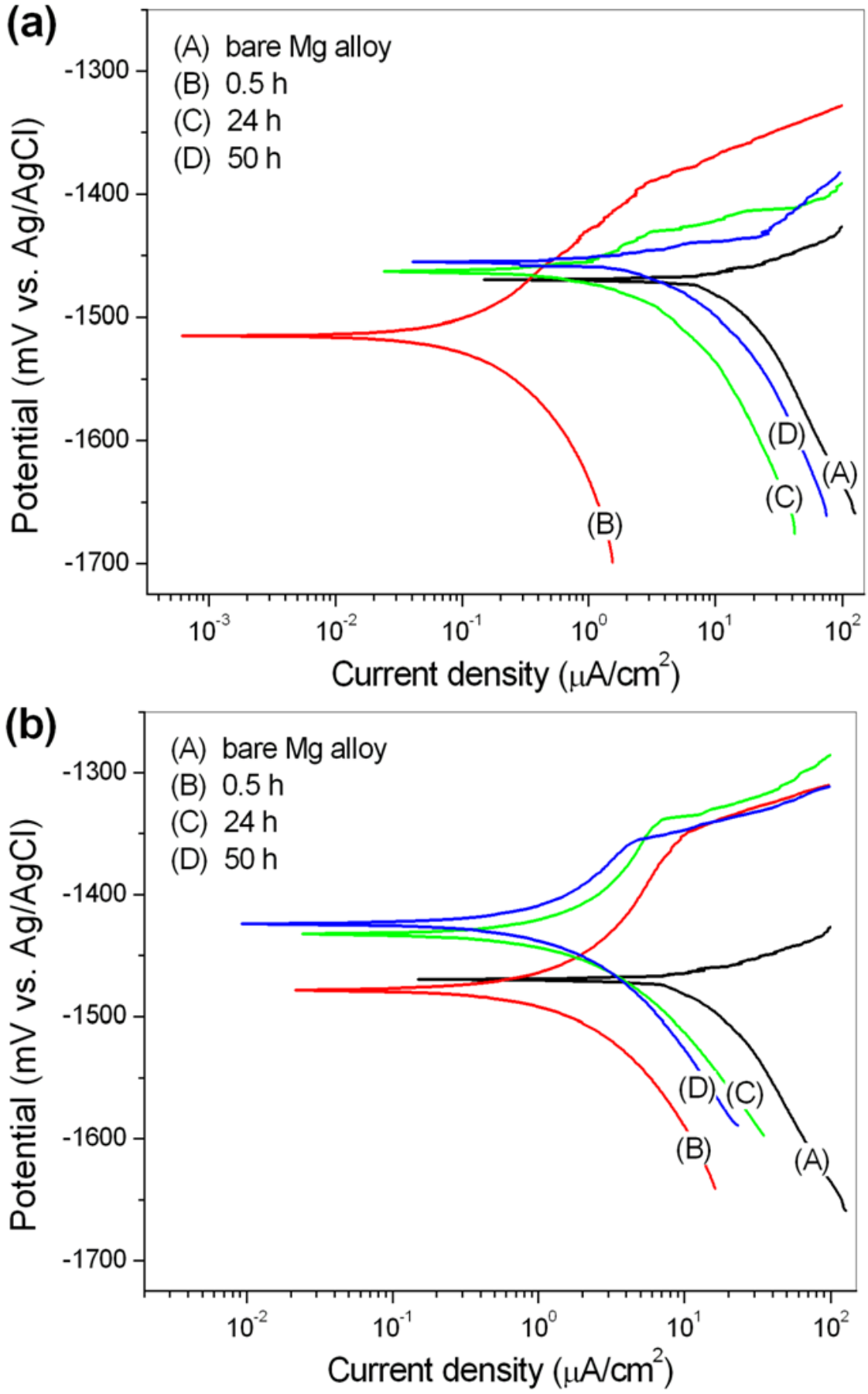

Figure 5 Potentiodynamic polarization behaviour of (a) MgO coating and (b) ZrO_2 coating on AM50 alloy in 0.1 M NaCl solution (after different durations of exposure).

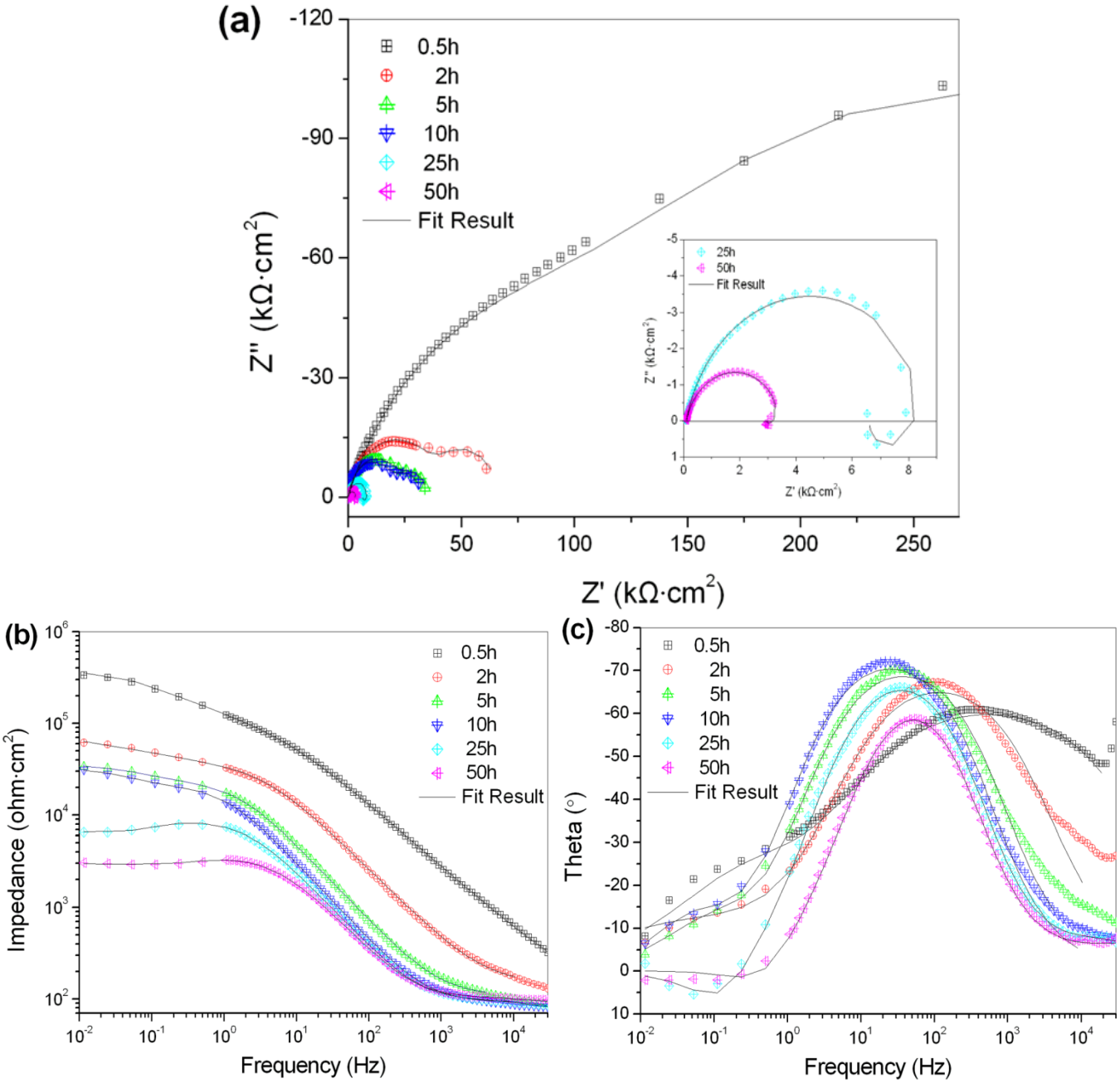

Figure 6 Experimental and fitting (a) Nyquist and (b, c) Bode plots of MgO coating at different immersion time in 0.1 M NaCl solution.

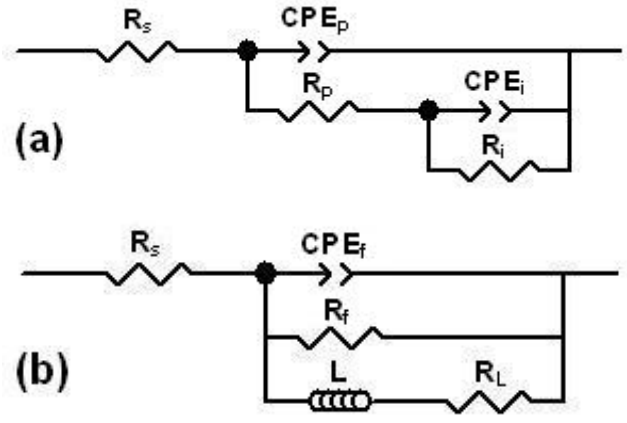

Figure 7 Equivalent circuits for fitting the impedance data of MgO coating on AM50B magnesium alloy (a) when the immersion time was up to 10 h; (b) when the immersion time was over 10 h.

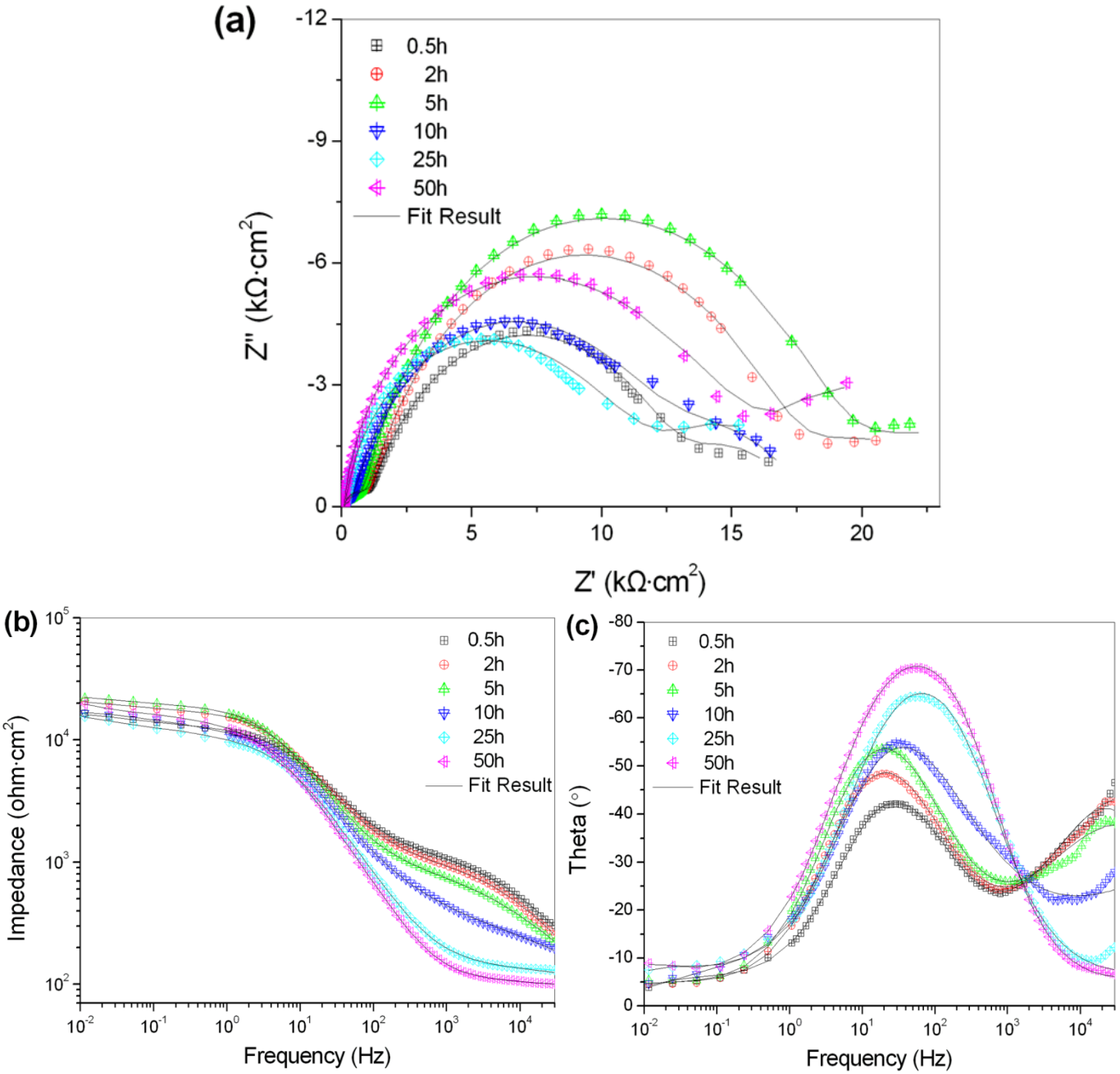

Figure 8 Experimental and fitting (a) Nyquist and (b, c) Bode plots of ZrO_2 coating at different immersion time in 0.1 M NaCl solution.

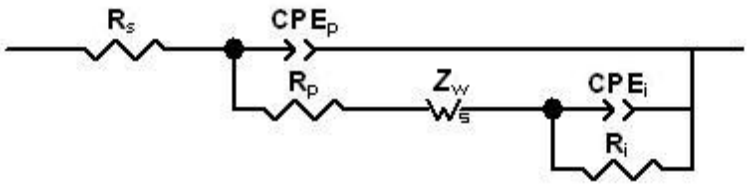

Figure 9 Equivalent circuits for fitting the impedance data ZrO_2 coating on AM50 magnesium alloy.

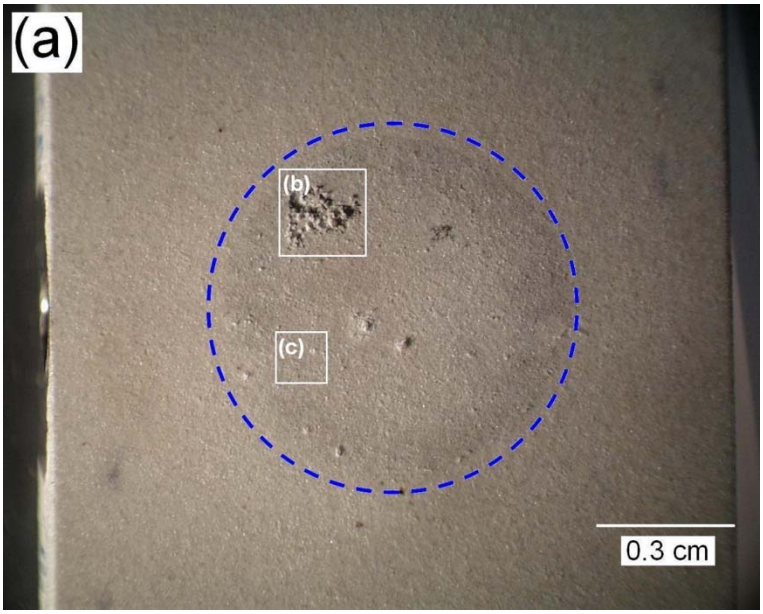

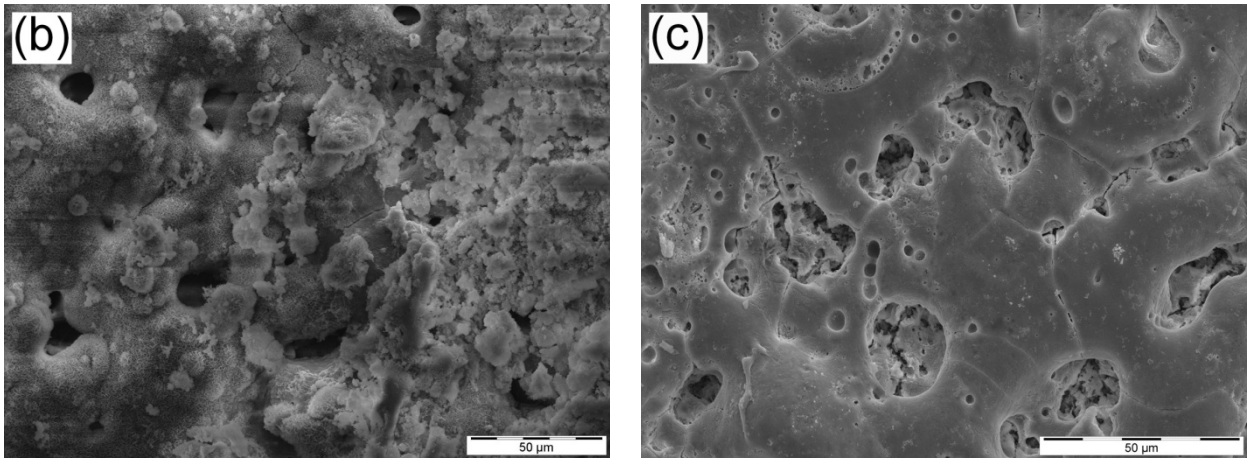

Figure 10 Surface appearances of MgO coating after 50 hours immersion in 0.1 M NaCl solution at pH 7 and a sequence of EIS tests performed during this immersion time:

(a) macroscopic morphology;
(b) higher magnification SEM micrograph showing the localized corrosion of the coating (region (b) in Figure 10(a));
(c) higher magnification SEM micrograph of region (c) in Figure 10(a).

The dashed circle in Figure 10(a) shows the exposure area during corrosion test.

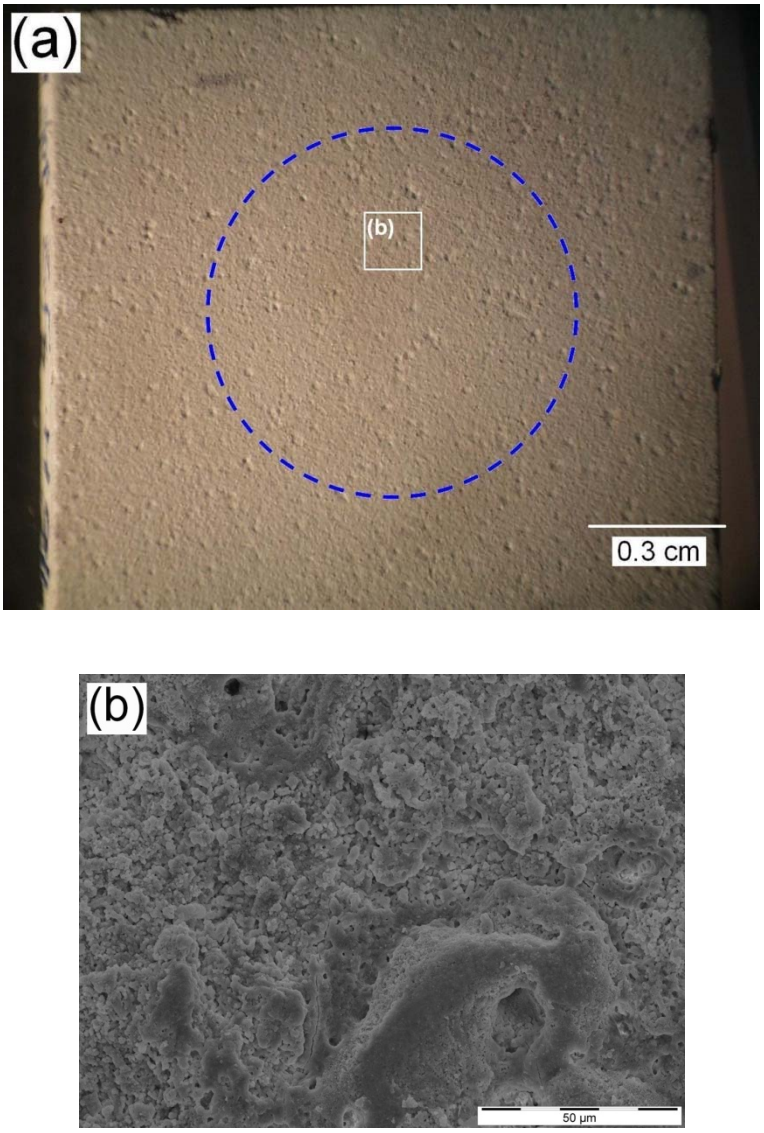

Figure 11 Surface appearances of ZrO_2 coating after 50 hours immersion in 0.1 M NaCl solution at pH 7 and a sequence of EIS tests performed during this immersion time:
(a) macroscopic morphology;
(b) higher magnification SEM micrograph of region (b) in Figure 11 (a).

The dashed circle in Figure 11(a) shows the exposure area during corrosion test.

Table 1 Electrochemical data from the polarization tests of the MgO coating on AM50 alloy in 0.1 M NaCl solution at different immersion times

Specimen	E_{corr} (mV vs. Ag/AgCl)	i_{corr} ($\mu A/cm^2$)	E_{bd} (mV vs. Ag/AgCl)
Bare alloy-0.5h	-1470	15	-------
MgO coated-0.5h	-1515	0.10	-1400
MgO coated-24h	-1462	5.6	-------
MgO coated-50h	-1455	11	-------

Table 2 Electrochemical data from the polarization tests of the ZrO_2 coating on AM50 alloy in 0.1 M NaCl solution at different immersion times

ZrO_2 coating	E_{corr} (mV vs. Ag/AgCl)	i_{corr} ($\mu A/cm^2$)	E_{bd} (mV vs. Ag/AgCl)
ZrO_2 coated-0.5h	-1478	2.0	-1350
ZrO_2 coated-24h	-1432	2.1	-1345
ZrO_2 coated-50h	-1424	2.1	-1358

Table 3 Fitting results of EIS plots of the MgO coating on AM50 magnesium alloy before 25 hours of immersion

Immersion time	$(CPE\text{-}T)_p$	$(CPE\text{-}P)_p$	R_p ($k\Omega\cdot cm^2$)	$(CPE\text{-}T)_i$	$(CPE\text{-}P)_i$	R_i ($k\Omega\cdot cm^2$)
0.5h	8.5×10^{-7}	0.70	130	5.5×10^{-6}	0.57	350
2h	2.3×10^{-6}	0.80	36	6.2×10^{-5}	0.48	52
5h	6.1×10^{-6}	0.84	24	2.0×10^{-4}	0.83	11
10h	9.0×10^{-6}	0.86	22	3.6×10^{-4}	0.91	10

Table 4 Fitting results of EIS plots of the MgO coating on AM50 magnesium alloy after 25 hours of immersion

Immersion time	$(CPE\text{-}T)_f$	$(CPE\text{-}P)_f$	R_f ($k\Omega\cdot cm^2$)	L *(H)*	R_L ($k\Omega\cdot cm^2$)
25h	1.2×10^{-5}	0.84	8.9	4.0×10^4	23
50h	1.4×10^{-5}	0.84	3.5	8.5×10^3	15

Table 5 Fitting results of EIS plots of the ZrO_2 coating on AM50 magnesium alloy

Immersion time	$(CPE\text{-}T)_p$	$(CPE\text{-}P)_p$	R_p ($k\Omega\cdot cm^2$)	Z_w ($k\Omega\cdot cm^2$)	$(CPE\text{-}T)_i$	$(CPE\text{-}P)_i$	R_i ($k\Omega\cdot cm^2$)
0.5h	7.8×10^{-7}	0.69	1.1	5.5	4.6×10^{-6}	0.80	11
2h	2.7×10^{-7}	0.80	0.61	9.2	4.4×10^{-6}	0.84	15
5h	1.5×10^{-6}	0.66	0.64	9.1	3.5×10^{-6}	0.88	17
10h	3.3×10^{-6}	0.56	0.19	6.9	3.7×10^{-6}	0.89	11
25h	1.2×10^{-5}	0.40	0.11	5.4	2.8×10^{-6}	0.94	13
50h	9.3×10^{-6}	0.42	0.09	6.3	3.2×10^{-6}	0.96	17